



저작자표시-비영리-변경금지 2.0 대한민국

이용자는 아래의 조건을 따르는 경우에 한하여 자유롭게

- 이 저작물을 복제, 배포, 전송, 전시, 공연 및 방송할 수 있습니다.

다음과 같은 조건을 따라야 합니다:



저작자표시. 귀하는 원저작자를 표시하여야 합니다.



비영리. 귀하는 이 저작물을 영리 목적으로 이용할 수 없습니다.



변경금지. 귀하는 이 저작물을 개작, 변형 또는 가공할 수 없습니다.

- 귀하는, 이 저작물의 재이용이나 배포의 경우, 이 저작물에 적용된 이용허락조건을 명확하게 나타내어야 합니다.
- 저작권자로부터 별도의 허가를 받으면 이러한 조건들은 적용되지 않습니다.

저작권법에 따른 이용자의 권리는 위의 내용에 의하여 영향을 받지 않습니다.

이것은 [이용허락규약\(Legal Code\)](#)을 이해하기 쉽게 요약한 것입니다.

[Disclaimer](#)

Role of ZMYND10
in the cytoplasmic preassembly
of dynein arms in multiciliated cells

Kyeong Jee Cho

Department of Medical Science

The Graduate School, Yonsei University

Role of ZMYND10
in the cytoplasmic preassembly
of dynein arms in multiciliated cells

Kyeong Jee Cho

Department of Medical Science

The Graduate School, Yonsei University

Role of ZMYND10
in the cytoplasmic preassembly
of dynein arms in multiciliated cells

Directed by Professor Heon Yung Gee

The Master's Thesis
submitted to the Department of Medical Science,
The Graduate School of Yonsei University
in partial fulfillment of the requirements for the degree of
Master of Medical Science

Kyeong Jee Cho

December 2017

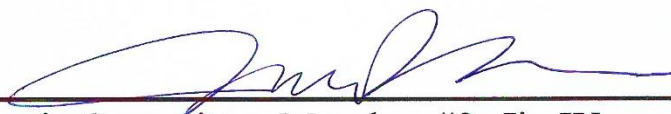
This certifies that The Master's Thesis
of Kyeong Jee Cho is approved.



Thesis Supervisor: Heon Yung Gee



Thesis Committee Member #1: Min Goo Lee



Thesis Committee Member #2: Jin Woong Bok

The Graduate School
Yonsei University

December 2017



ACKNOWLEDGEMENTS

第一 먼저, 藥理學 教室에 있는 동안 研究에 邁進할 수 있도록 아낌없는 激勵과 指導를 해 주신 指導敎授님이신 지현영 敎授님께 眞心으로 感謝 드립니다. 敎授님의 仔細한 指導 德分에 제가 發展하는 값진 時間을 보낼 수 있었습니다. 그리고 김경환 敎授님, 안영수 敎授님, 김동구 敎授님, 이민구 敎授님, 박경수 敎授님, 김철훈 敎授님, 김주영 敎授님, 김형범 敎授님께도 感謝 드립니다. 敎授님들의 가르침 德分에 藥理學 教室에서 研究에 入門할 수 있었고, 많은 가르침을 얻게 되었습니다. 또한, 바쁘신 中에 저의 學位 論文을 審査해 주신 복진웅 敎授님께도 感謝 드립니다.

碩士 課程 동안 함께 生活하면서 도움을 주신 많은 분들께도 感謝의 말씀 傳합니다. 于先, 實驗室의 바른 雰圍氣를 이끌어주신 217호의 기둥 같은 김연정 先生님, 바쁘신 渦中에도 뭐든지 親切하게 알려주신 노신혜 先生님, 그리고 저희 랩에 단비처럼 오신, 제가 依支를 많이 한 김혜연 先生님 感謝합니다. 先生님들의 助言과 應援이 힘이 많이 되었습니다. 셀을 아낌 없이 나눠주신 신동훈 先生님도 感謝합니다. 마지막 한 해 동안 랩 치프로서 두루두루 살피느라 苦生이 많으셨던 김지윤 先生님, 고운 데이터 그림들로 저의 本보기가 되었던 학이 언니도 感謝합니다. 힘들고 고될 때 마다 언제나 큰 慰勞가 되어주신 소원 先生님, 그리고 최성경 先生님, 윤지훈 先生님께도 感謝 드립니다. 電話機 옆자리에서 苦生 많았던, 卒業 同期 준석 先生님, 가벼울 땐 가볍고 眞摯할 때는 한 없이 眞摯한 難聽인 척 하는 영익이도 고맙습니다. 入學해서부터 卒業 때까지 繼續 막내이지만 옆자리에서 묵묵히 잘 챙겨준 세영이도 고맙습니다. 요즘 들어 實驗에 날개가 돋친 듯한 요준 先生님, 저의 죽은 쥐를 대신 잡아주는, 언제나 나이스한 정훈 先生님에게도 感謝함을 전합니다. 지금은 實驗室에 계시지 않지만, 入學 하자마자 제가 適應하는 데에 많은 도움을 주셨던, 뒷자리 先輩님들이신 정은석 先生님과 박형순 先生님도 感謝합니다. 전익현 先生님, 김한상 先生님, G0의 世界를 알려주고 가신 수민 언니, 그리고 저의 直屬 先輩로 랩 生活에 도움을 많이 준 윤이 오빠에게도 이렇게 紙面으로나마 感謝 人事를 傳합니다.

恒常 저를 믿어주시고 힘이 되어주시는 사랑하는 父母님, 感謝합니다. 每週 試驗과 死鬪를 벌이는 동생 윤정이에게도 고맙다고 傳하고 싶습니다.

마지막으로 여기에 일일이 言及하지 못한, 그 동안 저를 아껴주고 챙겨주신 모든 분들께 다시 한 번 眞心으로 感謝하다는 말씀을 드립니다.

곧 새로운 出發을 準備하는 제가 社會에 나가 한 層 더 成長하여 그 恩惠에 報答하는 사람이 되겠습니다.

感謝합니다.

TABLE OF CONTENTS

ABSTRACT	1
I. INTRODUCTION	3
II. MATERIALS AND METHODS	6
1. Mice.....	6
2. β -Galactosidase staining.....	6
3. Histology.....	6
4. TEM analysis.....	7
5. Videomicroscopy of ependymal cilia in mice.....	7
6. Antibodies.....	8
7. mTEC cultures.....	8
8. Immunofluorescence analysis.....	9
9. RNA isolation.....	9
10. RNA sequencing.....	10
11. Cell culture and transfection.....	10
12. Immunoblotting.....	10
13. Immunoprecipitation.....	10
14. GST pulldown assay.....	11
15. Protein stability assay.....	11
16. Statistical analysis.....	12
III. RESULTS	13
1. <i>Zmynd10</i> ^{-/-} mice recapitulate human PCD phenotypes.....	13



2. Loss of Zmynd10 causes axonemal ODA and IDA defects·····	19
3. Transcription levels of ODA and IDA components are unaltered in <i>Zmynd10</i> ^{-/-} mice·····	22
4. ZMYND10 forms a cytoplasmic protein complex·····	24
5. ZMYND10 stabilizes the cytoplasmic protein complex and regulates the preassembly of the dynein arm in the cytoplasm·····	28
6. ZMYND10 stabilizes LRRC6 and dynein intermediate chain proteins·····	31
IV. DISCUSSION ·····	35
V. CONCLUSION ·····	37
REFERENCES ·····	38
ABSTRACT (in Korean) ·····	42
PUBLICATION LIST ·····	44

LIST OF FIGURES

Figure 1.	Generation and validation of <i>Zmynd10</i> targeted alleles.....	15
Figure 2.	ZMYND10 antibody generation and validation.....	16
Figure 3.	<i>Zmynd10</i> ^{-/-} mice are runted, and develop hydrocephalus and/or situs inversus.....	17
Figure 4.	<i>Zmynd10</i> ^{-/-} mice exhibit phenotypes consistent with motile cilia defects.....	18
Figure 5.	<i>Zmynd10</i> ^{-/-} mice exhibit ODA and IDA defects.....	20
Figure 6.	ZMYND10 does not regulate mRNA expression of dynein arm components.....	23
Figure 7.	ZMYND10 forms a cytoplasmic protein complex	25
Figure 8.	ZMYND10 interacts with cytoplasmic proteins.....	27
Figure 9.	Dynein arm subunits and interaction partners of ZMYND10 are downregulated in <i>Zmynd10</i> ^{-/-} mice.....	29
Figure 10.	ZMYND10 stabilizes LRRC6 and DNAI1, an intermediate chain protein of ODA.....	32
Figure 11.	DNAI2 is stabilized by coexpression of both DNAI1	

and ZMYND10.....33

Figure 12. Function of ZMYND10 in the cytoplasmic
preassembly of dynein arms.....34

LIST OF TABLES

Table 1.	List of primers used for genotyping of Zmynd10 alleles.....	14
-----------------	--	----

ABSTRACT

**Role of ZMYND10 in the cytoplasmic preassembly
of dynein arms in multiciliated cells**

Kyeong Jee Cho

*Department of Medical Science
The Graduate School, Yonsei University*

(Directed by Professor Heon Yung Gee)

ZMYND10 is a cytoplasmic protein that causes primary ciliary dyskinesia (PCD) when mutated. PCD is characterized by respiratory symptoms and situs inversus, which is observed in 50% of patients. Up to now, 34 genes have been identified as the causative genes of PCD, and most of them are found in the structural components of cilia. ZMYND10 is one of the causative genes and present in cytoplasm of multiciliated cells. However, its function is not clearly identified.

Therefore, we examined by generating a mouse model. *Zmynd10*^{-/-} mice had growth retardation compared to wild type littermates, and could not survive more than 30 days. *Zmynd10*^{-/-} mice showed typical PCD-like phenotypes including hydrocephalus and laterality defects. Although the morphology and 9 + 2 axoneme structure of motile cilia as well as ciliogenesis remained normal, both outer and inner dynein arms were missing in motile cilia of *Zmynd10*^{-/-} mice, indicating that the absence of dynein arms is the primary cause of ciliary defects observed in *Zmynd10*^{-/-} mice.

To find the molecular mechanism of missing dynein arms in *Zmynd10*^{-/-} mice, we first performed RNA sequencing. mRNAs of dynein arm components were not changed in *Zmynd10*^{-/-}, suggesting that ZMYND10 does not regulate transcription of

dynein arms. ZMYND10 interacted with DYX1C1, C21ORF59 and LRRC6 which cause PCD, if defective, and also with IQUB, TCTEX1D1, DNAI1, and DNAI2 in cytoplasm. Protein levels of dynein arm components and interacting factors were significantly reduced in *Zmynd10*^{-/-} testis and trachea, whereas mRNAs of them were not downregulated in *Zmynd10*^{-/-} mice, indicating ZMYND10 regulates interactors and dynein arms at the protein level. To confirm this, we performed protein stability assay which showed that LRRC6 and DNAI1 are more stable when they are coexpressed with ZYMND10 compared to when they are expressed alone. DNAI2 was not stabilized when coexpressed with ZMYND10 alone, but was stabilized by coexpression with both DNAI1 and ZMYND10. This suggests that ZMYND10 stabilizes DNAI1, which subsequently stabilizes DNAI2.

In conclusion, our results suggest that ZMYND10 is necessary for motile cilia function. Moreover, ZMYND10 forms a cytoplasmic complex that regulates cytoplasmic preassembly of the dynein intermediate chain proteins.

Key words: motile cilia, primary ciliary dyskinesia (PCD), dynein arm, cytoplasmic preassembly, ZMYND10

Role of ZMYND10 in the cytoplasmic preassembly of dynein arms in multiciliated cells

Kyeong Jee Cho

*Department of Medical Science
The Graduate School, Yonsei University*

(Directed by Professor Heon Yung Gee)

I. INTRODUCTION

Primary Ciliary Dyskinesia (PCD) is an autosomal recessive disorder that occurs due to abnormal ciliary motility. It results from abnormal structures of motile cilia present in various parts of the body. Chronic respiratory diseases such as chronic cough and chronic sinusitis, and infertility are the main symptoms in PCD patients.^{1,2} Situs inversus totalis due to defects of the embryonic nodal cilia is present in 50% of the total patients.³ Up to date, about 34 genes have been identified as the causative genes for PCD, and mutations in these genes are known to account for up to 70% of PCD.³ PCD is caused by a mutation in the genes that encode the dynein arm or a structure that supports it. Most of these are components of motile ciliary structures such as outer dynein arm (ODA), inner dynein arm (IDA), radial spoke, and NDRC.

Motile cilia has a structure similar to that of flagella, and is found in a variety

of species. The motile cilia are cell organelles protruding out of the cell by a structure consisting of microtubules. The '9 + 2' axoneme forms the structure of cilia. Motile cilia get motility by the dynein arm, a type of motor protein attached to the microtubules. The motile cilia are specifically present in epithelial cells such as respiratory, ventricular, and fallopian tubes, and they are involved in functions such as mucus migration and cerebrospinal fluid circulation. There are dozens to hundreds of motile cilia in one cell.

Dynein arm is a massive multisubunit protein complex containing light, intermediate, and heavy chains.⁴ The completeness of the components of the heavy chain determines the ability of the dynein arm to function as a molecular motor, because it has an ATPase activity that provides the force to move between the microtubules. PCD-related genes include dynein arm components such as DNALI1, DNAI1, DNAI2, DNAH5 and DNAH6.^{5,6,7,8,9,10}

Dynein arm is known to be preassembled in the cytoplasm prior to docking to the motile cilia and docking in the surrounding microtubules. The detailed mechanism is not yet well known.¹¹ Dynein axonemal assembly factors (DNAAFs) are involved in assembly, and their mutations are known to be associated with PCD. Currently, there are four DNAAFs: LRRC50 (DNAAF1), KTU (DNAAF2), DNAAF3 and DYX1C1 (DNAAF4). DNAAFs are known to work with chaperone complexes, which serve to induce heavy chains to fold properly and facilitate assembly with the intermediate chains. Thus, without DNAAFs, a defect in ODA and IDA occurs in axoneme.^{12,13,14,15}

Mutations in ZMYND10, LRRC6, C21ORF59, ARMC4, and HEATR2 are also known to cause PCD.^{16,17,18,19,20,21,22} These also cause loss of ODA or IDA.^{21, 22,23,24} The exact function of proteins and their relationship to DNAAFs are not well known, but they appear to work at different stages of preassembly of dynein arms, or function in an ODA or IDA-specific manner.

ZMYND10 has myeloid, nervy and DEAF-1 (MYND)-type zinc finger domain at the C-terminus that is involved in protein-protein interactions.²⁵ ZMYND10 is found more in ciliated than in non-ciliated cells,²⁶ and is predominantly

expressed in motile ciliated tissue. ZMYND10 interacts with LRRC6, but it is not known how it functions in motile ciliated cells. In this study, we generated *Zmynd10*^{-/-} mice, which recapitulate phenotypic aspects of human PCD, including defects of ODA and IDA. In addition, DNAI1 and DNAI2, which are components of ODA, decreased in *Zmynd10*^{-/-} mice. ZYMND10 facilitated the assembly of the intermediate chains by binding to DNAI1 and stabilizing it. Our data suggest that ZMYND10 plays a role in the preassembly of dynein arms by regulating dynein arm components at the protein level rather than at the mRNA level and facilitating assembly with cytoplasmic protein complexes.

II. MATERIALS AND METHODS

1. Mice

The experimental protocol was reviewed and approved by the Animal Care Committee of Yonsei University College of Medicine. Targeted *Zmynd10*^{tm1(KOMP)Wtsi} embryonic stem cells were obtained from the Knockout Mouse Project Repository and injected into blastocysts. Chimeric mice were bred with C57BL/6J mice to establish germline transmission. Wild-type littermates were used as controls for *Zmynd10*^{-/-} mice.

Genotyping was performed by standard PCR using the primers indicated in Table 1.

2. β -Galactosidase staining

P14 mice were sacrificed and testes and lungs were dissected. After three washes with phosphate-buffered saline (PBS), the tissue was fixed in 4% paraformaldehyde (PFA)/0.02% NP-40 for 2 h at room temperature and permeabilized with 0.02% NP-40 in PBS for 1 h. Samples were incubated overnight at 37°C in X-gal staining solution composed of 5 mM $K_3Fe(CN)_6$, 5 mM $K_4Fe(CN)_6$, 2 mM $MgCl_2$, 0.01% sodium deoxycholate, 0.02% NP-40, and 1 mg/ml X-gal in PBS. They were then washed three times with PBS for 5 min each and post-fixed with 4% PFA for 24 h before embedding with paraffin. Sections cut at a thickness of 10 μ m were deparaffinized and rehydrated through a graded series of ethanol followed by counterstaining with Nuclear Fast Red (Vector Laboratories, Burlingame, CA, USA).

3. Histology

Lung and snout tissue specimens were fixed with 4% paraformaldehyde for 24 h. To decalcify the snout tissues, 0.5M EDTA solution (pH 8.0) was used. The tissues were immersed in the EDTA solution for about 3-4 weeks. The solution was changed

once every three days. Tissues were embedded in a paraffin block, sectioned at a thickness of 5 μm , and stained with hematoxylin and eosin, and Alcian blue staining reagent for histologic examination.

4. TEM analysis

The trachea of *Zmynd10*^{+/+} and *Zmynd10*^{-/-} mice at P10 were dissected and fixed in 2.5% glutaraldehyde, 1.25% PFA, and 0.03% picric acid in 0.1 M sodium cacodylate buffer (pH 7.4) overnight at 4°C. They were washed in 0.1M phosphate buffer, postfixed with 1% OsO₄ dissolved in 0.1M PBS for 2hr, dehydrated in ascending gradual series (50 ~ 100%) of ethanol and infiltrated with propylene oxide. Specimens were embedded by Poly/Bed 812 kit (Polysciences). After pure fresh resin embedding and polymerization at 65°C oven (TD-700, DOSAKA, Japan) for 24hr. Sections of about 200~250 nm thickness were initially cut and stained with toluidine blue (sigma, T3260) for light microscope. 70 nm thin section were double stained with 6% uranyl acetate (EMS, 22400 for 20 min) and lead citrate (Fisher, for 10 min) for contrast staining. These sections were cut by LEICA EM UC-7 (Leica Microsystems, Austria) with a diamond knife (Diatome) and transferred on copper and nickel grids. All of the thin sections were observed by transmission electron microscopy (JEM-1011, JEOL, Japan) at the acceleration voltage of 80kV.

5. Videomicroscopy of ependymal cilia in mice

P10 mice were deeply anesthetized and then decapitated. The brain was rapidly removed and immersed in ice-cold Dulbecco's Modified Eagle's Medium (DMEM, Invitrogen) supplemented with 10% fetal bovine serum (FBS, Sigma-Aldrich). Sagittal sections were cut at a thickness of 150 μm by using a vibratome (VT1200S, Leica). Sections from the third ventricle were visualized on an Axio Observer A1 microscope with a 63 \times phase contrast objective lens (LD Plan-Neofluor 0.75 Corr Ph2 M27; Carl Zeiss) equipped a high-speed charge-coupled device camera (optiMOS sCMOS; QImaging, Surrey). Movies were acquired at 100 frames per

second.

6. Antibodies

A polyclonal antibody recognizing the C-terminal sequence (amino acids 339–362, DRLERENKGKWQAIAKHQLQHVFS) of mouse ZMYND10 was recovered from rabbit injected with the corresponding antigen (AbFrontier). LRRC6 and DNAH5 antibodies have been previously described.^{31, 32} Antibodies against DNAI2 (H00064446-M01); REPTIN (ab89942); DNAH7 (NBP1-93613); DNAI1 (SAB4501181); IQUB (HPA020621); TCTEX1D1 (HPA028420); acetylated α -tubulin (T7451 and 5335S); FLAG (#8146; Myc (#2276); C21ORF59 (sc-365792); β -actin (sc-1615) were purchased from commercial sources. Secondary antibodies were purchased from Invitrogen and Santa Cruz Biotechnology for immunofluorescence analysis and immunoblotting, respectively.

7. mTEC cultures

mTECs were isolated from *Zmynd10*^{+/+} and *Zmynd10*^{-/-} mice at P14 as previously described.³³ Briefly, cells were isolated by overnight digestion with pronase (Roche Diagnostics) at 4°C and then separated from contaminating fibroblasts by incubation in mTEC basal medium on a Primaria cell culture plate (Corning Inc.) for 3–4 h. mTECs were seeded in collagen-coated apical chambers of transwell permeable supports (0.4 μ m polyester membrane; Corning Inc.). Proliferation medium was applied to the apical and basal chambers of the well and cells were cultured at 37°C in 5% CO₂.³⁴ For air-liquid interface (ALI) culture conditions, the medium was removed from the apical chamber when mTECs became confluent and differentiation medium was added to the basal chamber.

8. Immunofluorescence analysis

Mouse tracheal epithelial cells (mTECs) grown on inserts were fixed in 4% PFA for 10 min and permeabilized with 0.1% Triton X-100 for 20 min at room temperature. Tracheal tissue was fixed in 4% PFA overnight at 4°C, embedded in a paraffin block, and cut into 5 µm sections that were mounted on slides, deparaffinized, and rehydrated through a graded series of ethanol. After rehydration, antigen retrieval was performed by boiling sections for 30 min in Retrieve-All Antigen unmasking system 1 (pH 8; BioLegend). Sections were permeabilized with 1% sodium dodecyl sulfate for 10 min at room temperature. mTECs and incubated in blocking buffer containing 10% donkey serum and 1% bovine serum albumin for 1 hr at room temperature. Samples were incubated overnight at 4°C with primary antibodies diluted in blocking buffer. After washes with PBS, samples were incubated with secondary antibodies and 4',6-diamidino-2-phenylindole (DAPI) for 30 min at room temperature, washed, and covered with mounting medium and cover slips. Images were obtained with a SP5X laser scanning microscope (Leica) or LSM 700 microscope (Carl Zeiss).

9. RNA isolation

Total RNA was isolated from testis (P31), lung (P14) and brain (P14) tissue obtained from *Zmynd10*^{+/+} and *Zmynd10*^{-/-} mice using a Qiagen RNA extraction kit (Qiagen, Valencia). Each tissue was homogenized and incubated at RT for 5 min. 200 µl of chloroform was added and incubate the mixture at RT for 2 min. Centrifuge the mixture 12,000 g for 15 min at 4°C, and then transfer aqueous phase to a fresh tube. 1 volume of RB1 buffer was added to the sample and mixed by inverting. Transfer the mixture to a mini spin column and centrifuge at ≥ 10,000 g for 30 seconds to allow RNA to bind to the membrane. Add 500 µl of SW1 buffer to the column and centrifuge at ≥ 10,000 g for 30 seconds. Subsequently, add 500 µl of RNW buffer to the column and centrifuge at ≥ 10,000 g for 30 seconds to wash RNA. Add 50 ~ 100 µl of free-water to the center of the membrane in the column to elute RNA. Incubate for 1 min. Centrifuge at ≥ 10,000 g for 1 min, and RNA is completely isolated.

10. RNA sequencing

RNA sequencing was performed by TheraGen EteX. Libraries were constructed with the TruSeq RNA Library Sample Prep kit (Illumina) and the enriched library was sequenced on an Illumina HiSeq 2500 system. Sequence reads were mapped against the mouse reference genome (NCBI GRCm38/mm10) and analysed using CLC Genomics Workbench v.9.0.1 software (CLC Bio, Cambridge, MA, USA).

11. Cell culture and transfection

HEK293T cells were maintained in DMEM supplemented with 10% FBS and penicillin (50 IU/ml)/streptomycin (50 µg/ml). HEK293T cells were seeded into 60mm dishes at 2.5×10^6 cells/well and incubated at 37 °C, 5% CO₂, overnight. The cells were transfected with plasmids using Lipofectamine PLUS reagent (Invitrogen) and standard protocol recommendations were used.

12. Immunoblotting

Testis samples from P14 mice were dissected in PBS and lysed in the lysis buffer [150 mM NaCl, 1 mM EDTA, 50 mM Tris-HCl (pH 7.4), 1% NP-40, and complete proteinase inhibitors]. Lysates were centrifuged at 13,200rpm for 10 min at 4°C, and the supernatant was used for immunoblotting. Total protein concentration was measured using Bradford Protein Assay. Protein samples were resolved on SDS-PAGE (4-12%) gels and gels were transferred onto nitrocellulose blotting membranes. Membranes were blocked with 5% skim milk for 30 min at room temperature. Primary antibodies were diluted in 5% skim milk and incubated for overnight at 4°C. After washing with TBST, membranes were incubated with secondary antibodies. Protein blots were visualized by using West pico chemiluminescent substrate or West femto maximum sensitivity substrate kit (Pierce). Immunoblotting was quantified by densitometry using ImageJ software (National Institutes of Health, Bethesda, MD, USA).

13. Immunoprecipitation

HEK293T cells were seeded into 6-well plates at 1×10^6 cells/well and incubated at 37 °C, 5% CO₂ incubator overnight. Cells were lysed in lysis buffer. For 500 µg of proteins, 400 µl of lysis buffer was added. An agarose bead covalently bounded to anti-FLAG M2 antibody or anti-c-Myc antibody (Sigma-Aldrich) was washed twice with lysis buffer, and 400 µl of lysis buffer and protein lysates was added. Lysate-bead/antibody conjugate mixture was incubated overnight at 4°C. After the end of the incubation, centrifuge the tubes, and remove the supernatant from beads. To remove non-specific binding, the beads were washed with lysis buffer 3~4 times. When the wash was end, 20 µl of 2x SDS buffer was added and samples were incubated at 37 °C for 30 min. After the elution, the elutes were analyzed by immunoblotting.

14. GST pulldown assay

mTECs were lysed in the lysis buffer. Lysates were centrifuged, and the lysate supernatants were supplemented with 900 µl of buffer prior to addition of 10 µg of each GST fusion protein. The mixture was incubated overnight at 4 °C. After the end of the incubation, samples were supplemented with 80 µl of glutathione-Sepharose and incubated at 4 °C for 4 hr. The glutathione-Sepharose was pelleted and washed for 3 times at 4 °C with wash buffer (phosphate-buffered saline containing 0.1% Triton X-100 and 100 mM β-mercaptoethanol) prior to resuspension in SDS sample buffer and SDS-PAGE. Samples are ready to run on a western blot.

15. Protein stability assay

Cycloheximide (C4859; Sigma-Aldrich) chase was used to assess the stability of LRRC6, DNAI1, and DNAI2. HEK293T cells were transfected with Myc-tagged LRRC6, DNAI1, or DNAI2 with or without FLAG-tagged ZMYND10; at 24 h post-transfection, cells were treated with 100 µg/ml cycloheximide to inhibit new protein synthesis. Cells were harvested at predetermined time points and LRRC6, DNAI1,

and DNAI2 levels were detected by Western blotting.

16. Statistical analysis

Data are presented as the means \pm standard error of the mean. Statistical analysis was performed with Student's t-test, followed by Tukey's multiple comparison using the GraphPad Prism software package (version 5.0). $P < 0.05$ was considered statistically significant.

III. RESULTS

1. *Zmynd10*^{-/-} mice recapitulate human PCD phenotypes

To investigate the function of *Zmynd10*, we generated mice with targeted deletion of the *Zmynd10* gene locus (Fig. 1A, B) with a lacZ-containing targeting cassette (*Zmynd10*^{tm1[KOMP]Wtsi}). β -Galactosidase staining of *Zmynd10*^{+/-} lung tissue on postnatal day (P)1 showed that *Zmynd10* is expressed in the bronchus and bronchioles, but not in alveoli (Fig. 1C, D). *Zmynd10* expression was also observed in spermatids and earlier-stage germ cells of the *Zmynd10*^{+/-} testes at P28 (Fig. 1E, F). Deletion of coding exons 2 to 11 yielded a *Zmynd10* null allele (*Zmynd10*^{-/-}), and the absence of ZMYND10 was proved by western blot of testes lysates (Fig. 2A) and immunofluorescence analyses of tracheal tissue (Fig. 2B and C).

Zmynd10^{-/-} mouse litters followed Mendelian ratios. They showed no gross abnormalities, revealing that loss of *Zmynd10* does not cause embryonic lethality; however, mutant mice were much smaller at P10, indicating growth retardation. All mutant died within 30 days of birth (Fig. 3A-C), with a mean survival of 14 days. *Zmynd10*^{-/-} mice developed hydrocephalus (Fig. 4A and B), observed by hematoxylin and eosin (H&E) staining, with the dilated cerebral ventricles and thinned cortical tissues (Fig. 4C-F). Moreover, 42% of *Zmynd10*^{-/-} mice showed lateral defects (Fig. 3D and E). Mucus congestion in *Zmynd10*^{-/-} mice was indicated by Alcian Blue staining of paranasal cavities, suggesting that mucociliary clearance is defective in *Zmynd10*^{-/-} mice (Fig. 4G and H). Mutant mice died before P20 did not show lung inflammation, whereas mutants which survived over P25, revealed inflammation in lung tissue evidenced by loss of alveolar structure, and collapse of the alveolar space (Fig. 4I and J). Taken together, these data showed that loss of *Zmynd10* causes defects consistent with PCD.

Table 1. List of primers used for genotyping of different Zmynd10 alleles

Primer	Sequence
Zmynd10-ex2F	TGGAGGAGCTTGGAAC TGAC'
Zmynd10-ex2R	GGAGGCAGACACAGTTAGGC
CSD-RAF5-F	ACACCTCCCCCTGAACCTGAAA
SR1	TGCTTTATTGTGCGAAAGGAAGAGGG

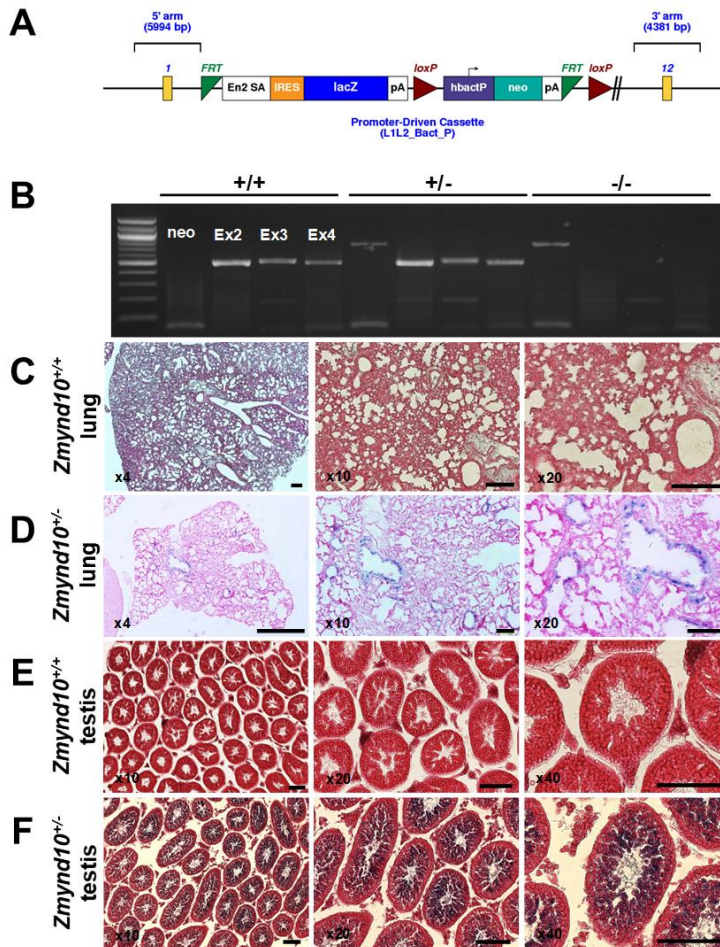


Figure 1. Generation and validation of *Zmynd10* targeted alleles. (A) Diagram of *Zmynd10* targeted allele. (B) Wild-type, heterozygous, and homozygous sex-matched littermates were genotyped by PCR based on the presence of the neomycin cassette, exon 2, exon3 or exon4. Wild-type allele was 529 bp, mutant allele was 764 bp. (C-F) X-gal staining of *Zmynd10* wild-type and heterozygote lung (C and D), and testis (E and F). Each sections were counterstained with nuclear fast red. (C and D) X-gal staining in a section of *Zmynd10*^{+/+} lung confirmed *Zmynd10* expression in the bronchiole. Scale bars, 200 μm. (E and F) X-gal staining revealed that *Zmynd10* was expressed from spermatocytes to spermatids in *Zmynd10*^{+/+} testis. Scale bars, 100 μm.

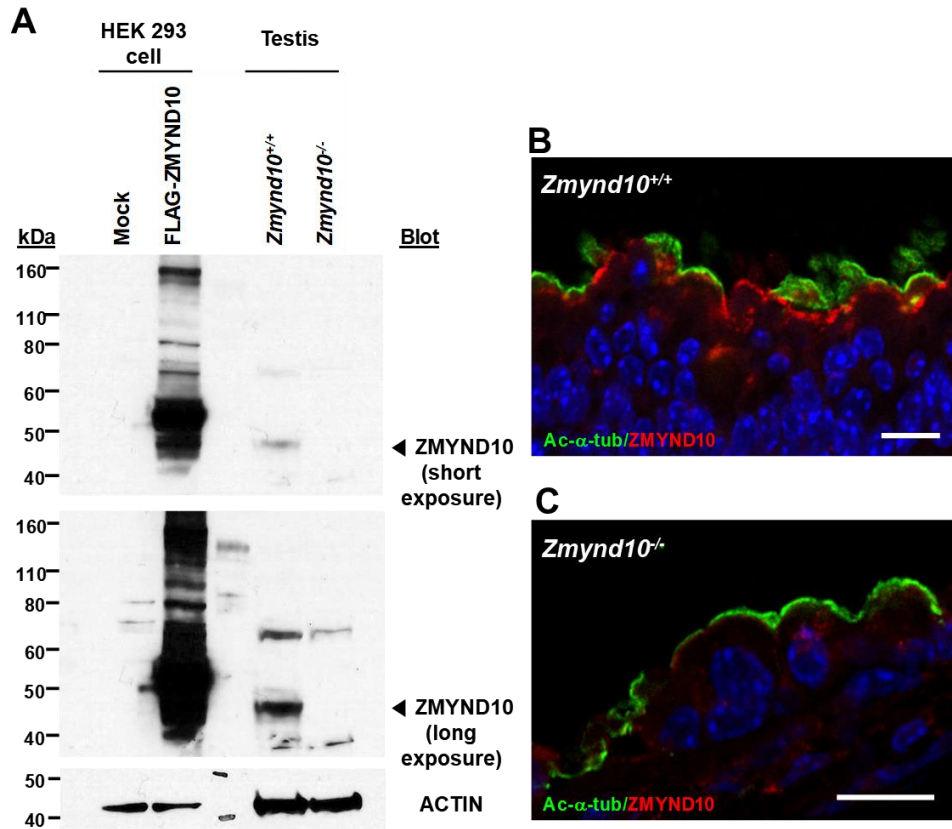


Figure 2. ZMYND10 antibody generation and validation. (A) Immunoblotting of lysates of HEK293 cells transfected with FLAG-ZMYND10 and of mouse testis. 50 μ g protein samples was used for the testis from *Zmynd10*^{+/+} and *Zmynd10*^{-/-} mice. ZMYND10 was approximately 50 kDa. (B and C) Immunofluorescence analysis of tracheal epithelium in *Zmynd10*^{+/+} (B) and *Zmynd10*^{-/-} (C) mice. ZMYND10 (red) was localized in apical membrane and not colocalized with acetylated- α -tubulin (green), a ciliary marker, in *Zmynd10*^{+/+} mouse trachea (B). However, ZMYND10 was not detected in *Zmynd10*^{-/-} (C). Scale bars, 10 μ m (B and C).

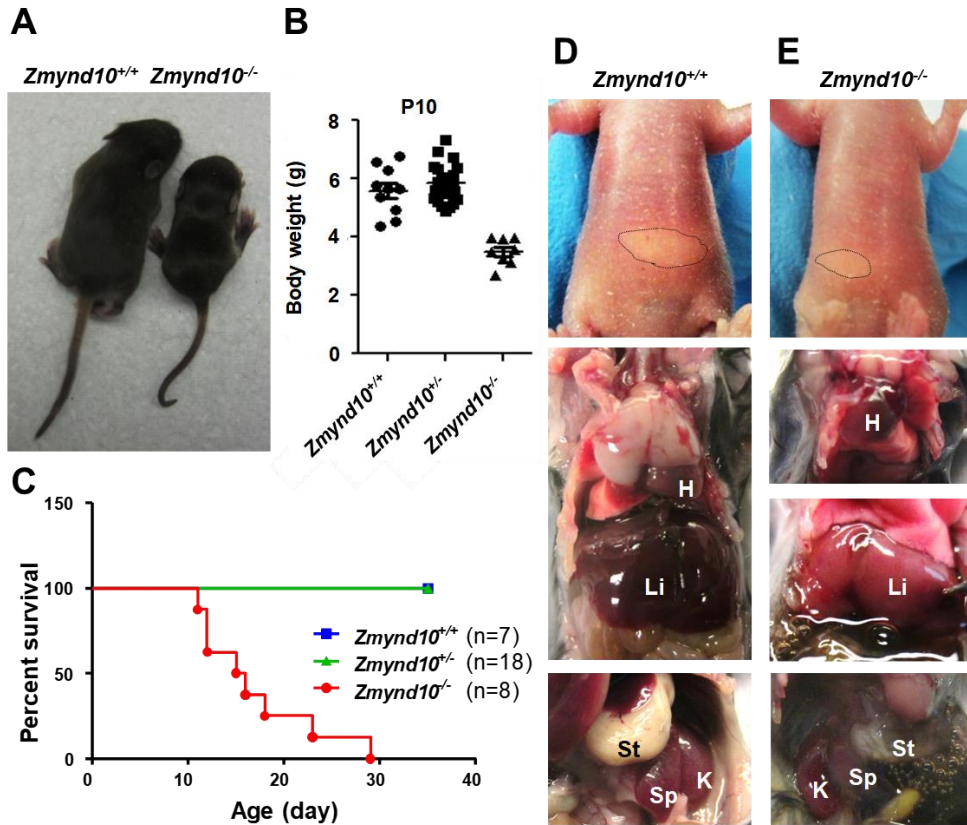


Figure 3. *Zmynd10*^{-/-} mice were runted, and developed hydrocephalus and/or situs inversus. (A) Picture of *Zmynd10* wild-type and homozygote. *Zmynd10*^{-/-} mice were notably smaller than *Zmynd10*^{+/+} sibling. (B) Body weight was quantified at the age of 10 days. *Zmynd10*^{-/-} mice exhibited severe growth retardation compared to *Zmynd10*^{+/+} or *Zmynd10*^{+/-} littermates. (C) Survival graph of the indicated genotypes and numbers (n). All of *Zmynd10*^{-/-} mice died within 30 postnatal days. (D and E) *Zmynd10*^{-/-} mice showed situs inversus, consistent with randomization of left-right body asymmetry (E). The locations of stomach, heart, liver, and spleen were indicated. The location of stomach, heart, liver and spleen was reversed in *Zmynd10*^{-/-} mouse (E). H, heart; K, kidney; Sp, spleen; St, stomach.

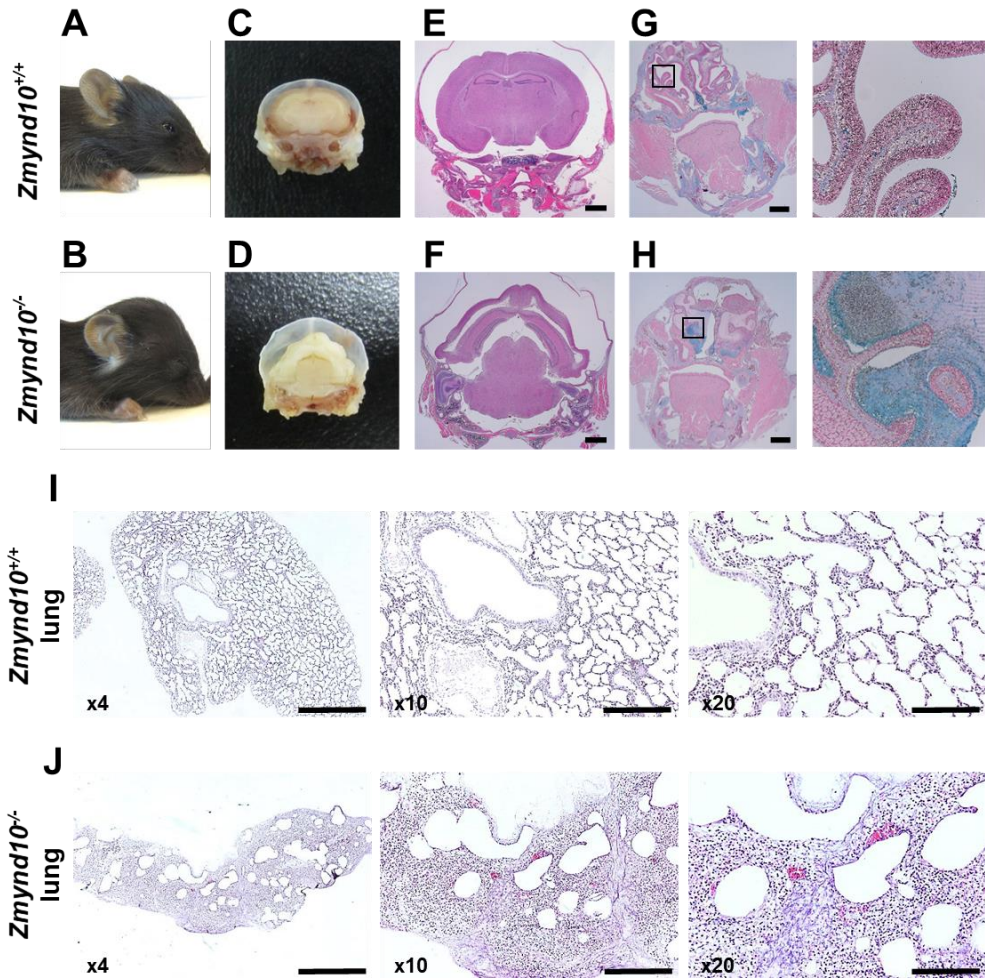


Figure 4. *Zmynd10*^{-/-} mice indicated phenotypes consistent with motile cilia defects. (A, B) *Zmynd10*^{-/-} mice showed severe hydrocephalus which resulted in typical head deformation. Scale bars, 1 mm. (C, D) Coronal brain sections exhibited enlarged ventricular cavity with reduced cortical tissue in *Zmynd10*^{-/-} mice. Scale bars, 1 mm. (E, F) H&E staining of coronal brain sections revealed enlarged ventricles in *Zmynd10*^{-/-} mice. (G, H) Alcian Blue staining of paranasal cavities revealed mucus congestion in *Zmynd10*^{-/-} mice. (I, J) H&E staining of lung sections at P30 demonstrated severe pulmonary inflammation in mutants. Original magnification, 40× (scale bar, 500 μm), 100×, and 200× (scale bar, 100 μm).

2. Loss of *Zmynd10* causes defects of axoneme ODA and IDA

Since the *Zmynd10*^{-/-} phenotype demonstrated defects in motile cilia, we observed ultrastructure of motile cilia by transmission electron microscopy (TEM). Tracheal cilia and basal bodies were abundant in tracheal epithelial cells of both *Zmynd10*^{+/+} and *Zmynd10*^{-/-} mice (Fig. 5A–D). Tracheal cilia analyzed in cross sections showed the typical 9+2 microtubular structure in both wild-type and *Zmynd10*^{-/-} mice (Fig. 5E and F). However, both ODA and IDA structures were defective in *Zmynd10*^{-/-} cilia (Fig. 5H), while they were present in the peripheral microtubules of *Zmynd10*^{+/+} mice (Fig. 5G).

We next observed the subcellular distribution of the ODA intermediate chain protein DNAI2 by immunofluorescence microscopy in mouse tracheal epithelial cells (mTECs) cultured at the air-liquid interface (ALI) for 14 days. In mTECs from *Zmynd10*^{+/+} mice, DNAI2 was detected in cilia and colocalized with acetylated α -tubulin (Fig. 5I; Left). However, expression of DNAI2 was remarkably reduced in the cytoplasm of mTECs from *Zmynd10*^{-/-} mice. When *Zmynd10* is absent, DNAI2 seemed to fail to move to motile cilia from cytoplasm (Fig. 5I; Right). Therefore, phenotypes observed in *Zmynd10*^{-/-} mice resulted from ciliary motility defect associated with the loss of axonemal ODA and IDA.

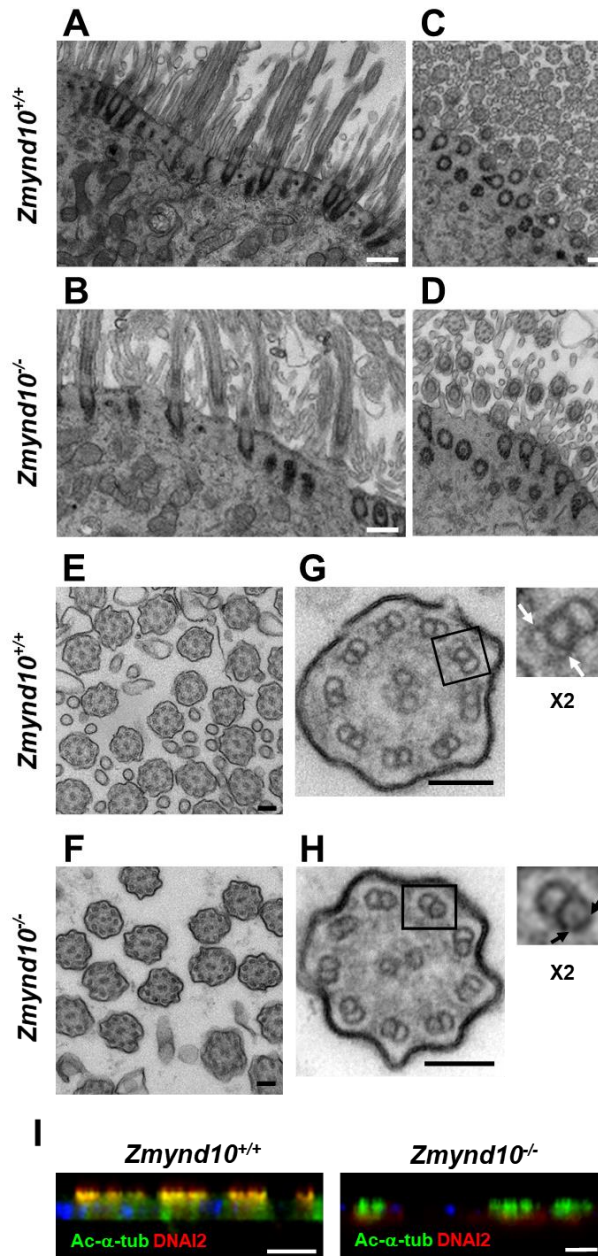


Figure 5. *Zmynd10*^{-/-} mice exhibit ODA and IDA defects. (A–D) Multiciliated cells from trachea of P14 *Zmynd10*^{+/+} and *Zmynd10*^{-/-} were analyzed by TEM. The number and morphology of cilia and basal bodies were almost same between *Zmynd10*^{+/+} (A, B) and *Zmynd10*^{-/-} (C, D) mice. Scale bars, 500 μ m. (E, F) TEM of motile cilia axonemes indicates normal 9+2 microtubule structures in both *Zmynd10*^{+/+} and

Zmynd10^{-/-} mice. Scale bars, 500 μ m. (G, H) In peripheral microtubule doublets of motile cilia in *Zmynd10*^{+/+} mice, ODAs and IDAs (white arrows) were observed (G), however, they were absent in that of *Zmynd10*^{-/-} mice (H, black arrows). Scale bars, 500 μ m. (I) In mTEC cultures at ALI day 14, acetylated- α -tubulin (green) and DNAI2 (red) expression was analyzed by immunofluorescence. In *Zmynd10*^{-/-} mTECs, DNAI2 did not colocalize with acetylated α -tubulin, indicating that ODAs were absent in motile cilia. Acetylated α -tubulin was expressed in both *Zmynd10*^{+/+} and *Zmynd10*^{-/-} mTECs, showing that loss of *Zmynd10* did not affect ciliogenesis. Scale bars, 10 μ m.

3. Transcript levels of ODA and IDA components are unaltered in *Zmynd10*^{-/-} mice

The mRNA levels of DNAH5, ODA heavy chain and DNALI1, ODA light chain proteins were downregulated by ZMYND10 knockdown in cultured human tracheal epithelial cells.¹⁸ We examined this in *Zmynd10*^{+/+} and *Zmynd10*^{-/-} mice by transcriptional profiling/RNA sequencing using total RNA isolated from testis, lung, and brain tissues. ODA and IDA components showed similar transcript levels both in mutant and wild-type mice (Fig. 6), indicating that the transcription of dynein arm components is not affected by Zmynd10.

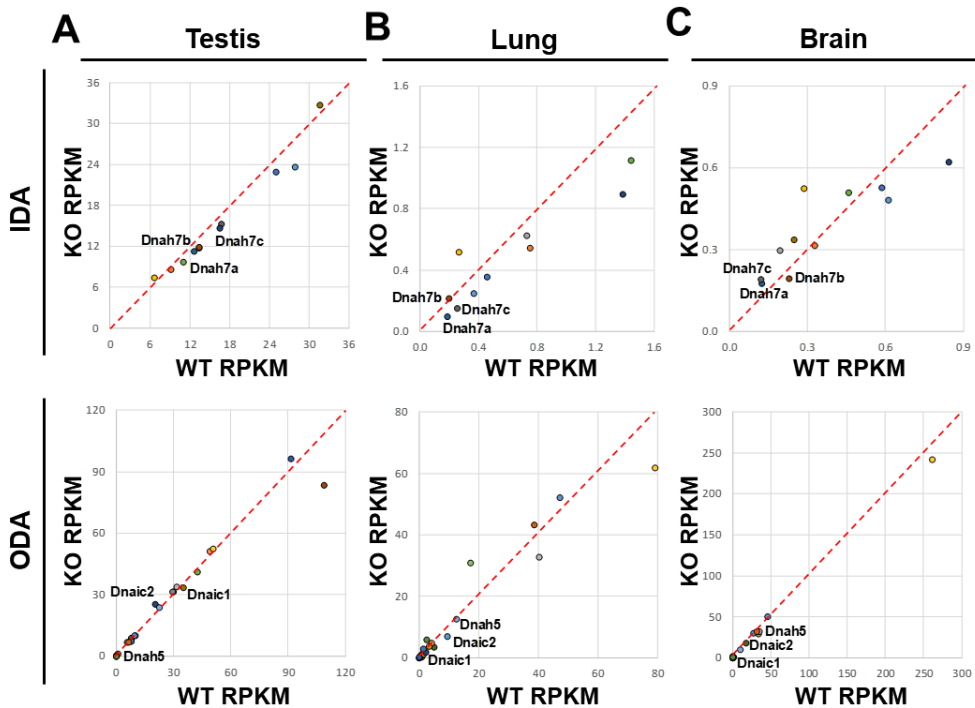


Figure 6. *Zmynd10* did not regulate mRNA expression of dynein arm components. (A-C) Graphs comparing reads per kilobase of transcript per million mapped reads (RPKM) of ODA and IDA components. Total RNAs were extracted from P21 testis (A), P14 lung (B), and P14 brain (C) tissue from *Zmynd10*^{+/+} and *Zmynd10*^{-/-} mice. The expression of most dynein arm components was similar between wild-type and mutant mice.

4. ZMYND10 forms a cytoplasmic protein complex

It was reported that ZMYND10 interacts with LRRC6.^{18, 19} Since both proteins are cytoplasmic, we examined whether they interact with other cytoplasmic proteins that are known to be defective in PCD by co-immunoprecipitation in HEK293T cells. ZMYND10 interacted with IQUB, TCTEX1D1, DYX1C1, DNAAF4, C21ORF59 and DNAI1 but not with DNAI2 (Fig. 8). Interaction of ZMYND10 with LRRC6, REPTIN (RUVBL2), which is essential for cilia motility,²⁷ and with C21ORF59 was confirmed with the glutathione S-transferase (GST) pulldown assay using lysates from mTECs (Fig. 7A). These protein interaction networks are shown in Fig. 7B. REPTIN and C21ORF59 expression in mTECs was also examined at ALI 14 by immunofluorescence microscopy. In *Zmynd10*^{-/-} mTECs, REPTIN and C21ORF59 signals were reduced remarkably (Fig. 7C and D). Our results show that ZMYND10 interacts with cytoplasmic proteins linked to PCD and that some interaction partners are reduced when Zmynd10 is absent.

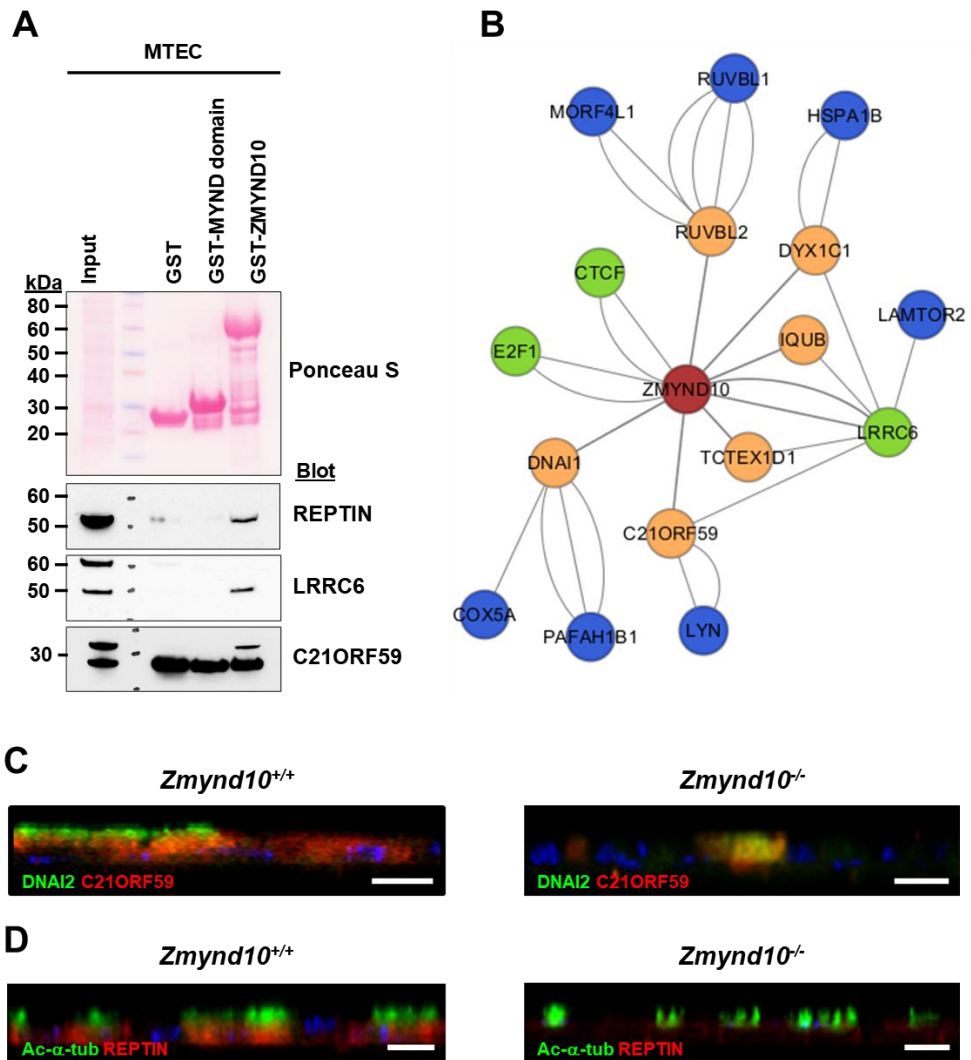


Figure 7. ZMYND10 formed a cytoplasmic protein complex. (A) GST pulldown assay of purified MYND domain of ZMYND10 or the full-length ZMYND10. REPTIN, LRRC6, and C21ORF59 in mTECs were pulled down by full-length ZMYND10 but not by the MYND domain alone. (B) Protein interaction network of ZMYND10 and its binding partners. Proteins in orange nodes were identified in this study. E2F1, CTCF, and LRRC6 (green nodes) were known interaction partners of ZMYND10. The first neighbors (blue nodes) of ZMYND10-interacting proteins were determined from a protein-protein interaction (PPI) network based on public data sources including GeneMANIA (<http://genemania.org/>, 190 references of PPI in human, 35 references of PPI in *Mus musculus*). (C) Immunofluorescence analysis of

DNAI2 (green) and C21ORF59 (red) in mTECs. In *Zmynd10*^{+/+} mTECs, C21ORF59 was observed in the cytoplasm whereas DNAI2 was mostly localized in cilia at ALI day 14 (C; Left). DNAI2 was completely missing from motile cilia, and DNAI2 and C21ORF59 were downregulated in *Zmynd10*^{-/-} mTECs (C; Right). Nuclei were stained with 4',6-diamidino-2-phenylindole (DAPI). Scale bars, 10 μ m. (D) Immunofluorescence analysis of acetylated α -tubulin (green) and REPTIN (red) in mTECs. REPTIN was localized in the cytoplasm in *Zmynd10*^{+/+} mTECs (D; Left), but was completely absent in *Zmynd10*^{-/-} cells (D; Right). Scale bars, 10 μ m.

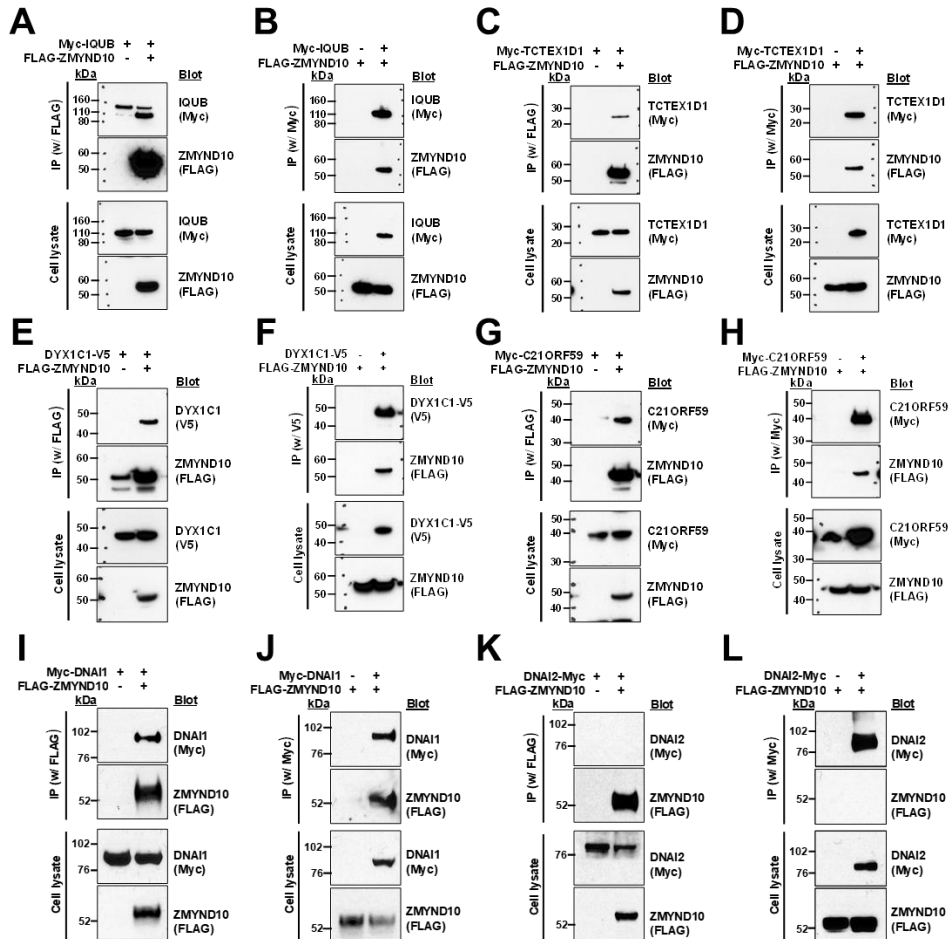


Figure 8. ZMYND10 interacted with cytoplasmic proteins. (A-L) Interactions between FLAG-tagged ZMYND10 and Myc-tagged IQUB (A and B), Myc-TCTEX1D1 (C and D), DYX1C1-V5 (E and F), Myc-C21ORF59 (G and H), Myc-DNAI1 (I and J), or Myc-DNAI2 (K and L). All constructs were co-transfected into HEK293T cells and lysates were coimmunoprecipitated with a FLAG antibody (A, C, E, G, I, and K) or a Myc antibody (B, D, F, H, J and L). The immunoblots indicated that antibodies did not show nonspecific bands. These results showed protein-protein interaction between ZMYND10 and IQUB, TCTEX1D1, DYX1C1, C21ORF59, or DNAI1 (A-J). However, ZMYND10 did not interact with DNAI2 (K and L).

5. ZMYND10 stabilizes the cytoplasmic protein complex and regulates the preassembly of the dynein arm in the cytoplasm

Our immunofluorescence results in mTECs demonstrated that protein levels of dynein arm components (Fig. 5I) and their interaction partners (Fig. 7C and D) were decreased in *Zmynd10*^{-/-} mice. To examine this in detail, we carried out immunoblotting using testis lysates. The levels of proteins interacting with ZMYND10 such as C21ORF59, IQUB, and LRRC6 as well as dynein arm components including DNAH7, DNAI1, and DNAI2 were decreased in *Zmynd10*^{-/-} mice (Fig. 9A and B). Immunofluorescence analysis of mouse tracheal tissue also confirms this. DNAH5, DNAI2, and IQUB signals were much weaker in *Zmynd10*^{-/-} than *Zmynd10*^{+/+} mice (Fig. 9C–E). The mRNA levels of dynein arm components were similar between *Zmynd10*^{+/+} and *Zmynd10*^{-/-} mice (Fig. 6). These data suggest that in the absence of Zmynd10, ODA and IDA are unstable, probably due to improper assembly. We assumed whether dysregulated transcription in *Zmynd10*^{-/-} mice resulted in the decrease in protein levels of ZMYND10-interacting factor. To inspect this speculation, we examined the transcript levels of these factors and of DNAAFs, which are involved in dynein arm assembly factor 3, by RNA sequencing. There were no differences in the mRNA levels of these proteins between *Zmynd10*^{+/+} and *Zmynd10*^{-/-} mice (Fig. 9F–H). These results reveal that ZMYND10 stabilizes dynein arm components and their interaction partners at the protein level but not at the transcript level.

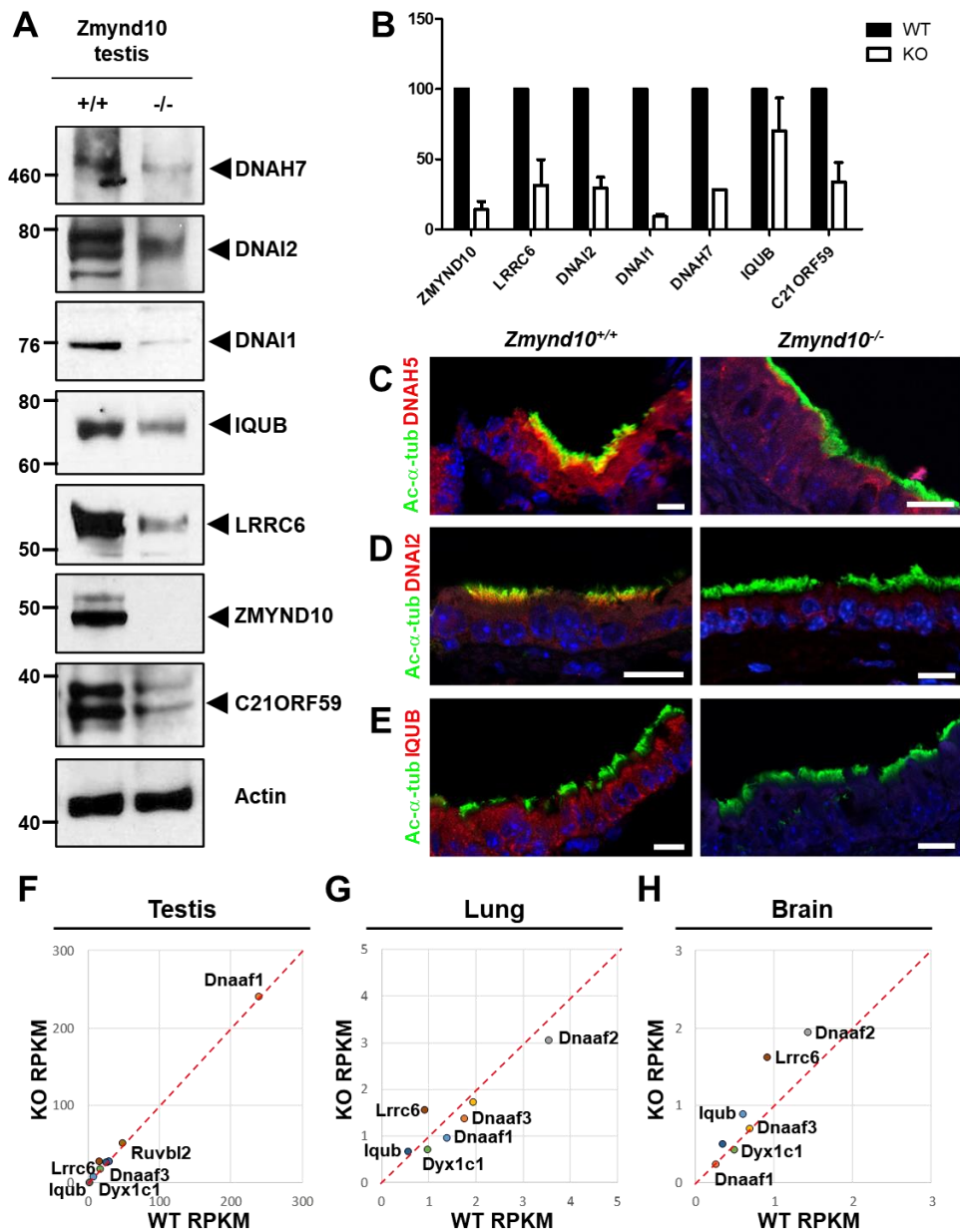


Figure 9. Dynein arm subunits and interaction partners of ZMYND10 were downregulated in *Zmynd10*^{-/-} mice. (A) Representative immunoblot analyses of DNAH7, DNAI2, DNAI1, IQUB, LRRC6, C21ORF59, and ZMYND10 in testis extracts from *Zmynd10*^{+/+} and *Zmynd10*^{-/-} mice. Intermediate chains of ODA and

interacting proteins were downregulated in *Zmynd10*^{-/-} mice. (B) Bar graphs represented band intensities of the blot shown in panel (A) and data represented the mean \pm SD of more than three independent experiments. (C–E) Tracheal multiciliated epithelia in *Zmynd10*^{+/+} and *Zmynd10*^{-/-} mice were analyzed by immunofluorescence analysis. (C) DNAH5 (red), an ODA heavy chain protein, localized to both cilia and cytoplasm of *Zmynd10*^{+/+} trachea and colocalized with acetylated α -tubulin, but was almost completely absent from *Zmynd10*^{-/-} trachea. DNAI2 (red) was present in both cilia and cytoplasm in *Zmynd10*^{+/+} trachea. However, DNAI2 expression was absent from *Zmynd10*^{-/-} trachea (D). IQUB (red), a cytoplasmic protein and ZMYND10 interaction partner, was not detectable in *Zmynd10*^{-/-} trachea (E). Scale bars, 10 μ m. (F–H) Graphs comparing RPKM values of dynein arm assembly factors and ZMYND10-interacting proteins in testis (F), lung (G), and brain (H) tissues of *Zmynd10*^{+/+} and *Zmynd10*^{-/-} mice. There was no difference in expression levels of these proteins between *Zmynd10*^{+/+} and *Zmynd10*^{-/-} mice.

6. ZMYND10 stabilizes LRRC6 and dynein intermediate chain proteins

We examined how ZMYND10 affects the stability of LRRC6, DNAI1, and DNAI2 in a heterologous system, to further examine whether ZMYND10 regulates dynein arms and its interaction partners at the protein level. LRRC6 and/or ZMYND10 were overexpressed in HEK293T cells, and treated with cycloheximide (100 μ g/ml) for up to 48 h to inhibit protein synthesis (Fig. 10A). Only 7.8% of LRRC6 remained after 48 h cycloheximide treatment. However, when LRRC6 was co-expressed with ZMYND10, this value was increased to 44.4% (Fig. 10B), indicating that ZMYND10 prevented LRRC6 degradation. Likewise, when co-expressed with ZMYND10, the amount of DNAI1 protein was increased from 31.0% to 56.9% (Fig. 10C and D). Otherwise, the stability of DNAI2, which does not interact with ZMYND10 (Fig. 8K and L), was unaffected when co-expressed with ZMYND10 (Fig. 10E and F). Given that both DNAI1 and DNAI2 levels were reduced in *Zmynd10*^{-/-} mice, we considered that ZMYND10 stabilized DNAI1, which stabilized DNAI2 in order. We compared the protein levels of DNAI2 co-expressed with DNAI1 without or with ZMYND10, to examine this hypothesis (Fig. 11). When co-expressed with both DNAI1 and ZMYND10, DNAI2 was much more stable compared to DNAI1 alone (Fig. 11). These results demonstrate that ZMYND10 stabilizes some of its interaction partners at the protein level and regulates the preassembly of intermediate chains by stabilizing DNAI1 (Fig. 12).

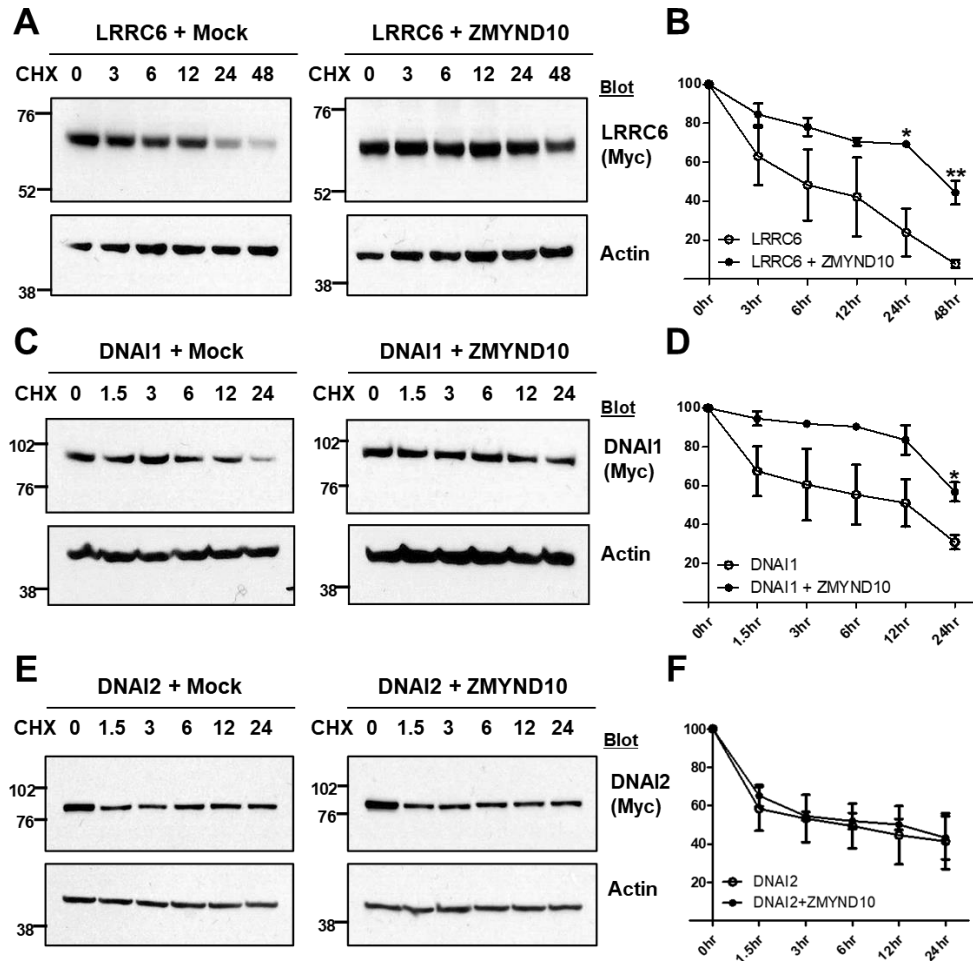


Figure 10. ZMYND10 stabilized LRRC6 and DNAI1, an intermediate chain protein of ODA. The stability of LRRC6, DNAI1, and DNAI2 was examined with the protein stability assay. Protein samples were harvested at indicated times after treatment with cycloheximide (100 μ g/ml). (A, B) Representative immunoblot of LRRC6 stability assay (A). The stability of LRRC6 was increased when co-expressed with ZMYND10 (B). (C, D) Representative immunoblot of DNAI1 stability assay (C). DNAI1 stability was increased when co-expressed with ZMYND10 (D). (E, F) Representative immunoblot of DNAI2 stability assay (E). Protein levels of DNAI2 were not affected by ZMYND10 coexpression (F). Data were representative of at least three independent experiments. * $P < 0.05$; ** $P < 0.005$.

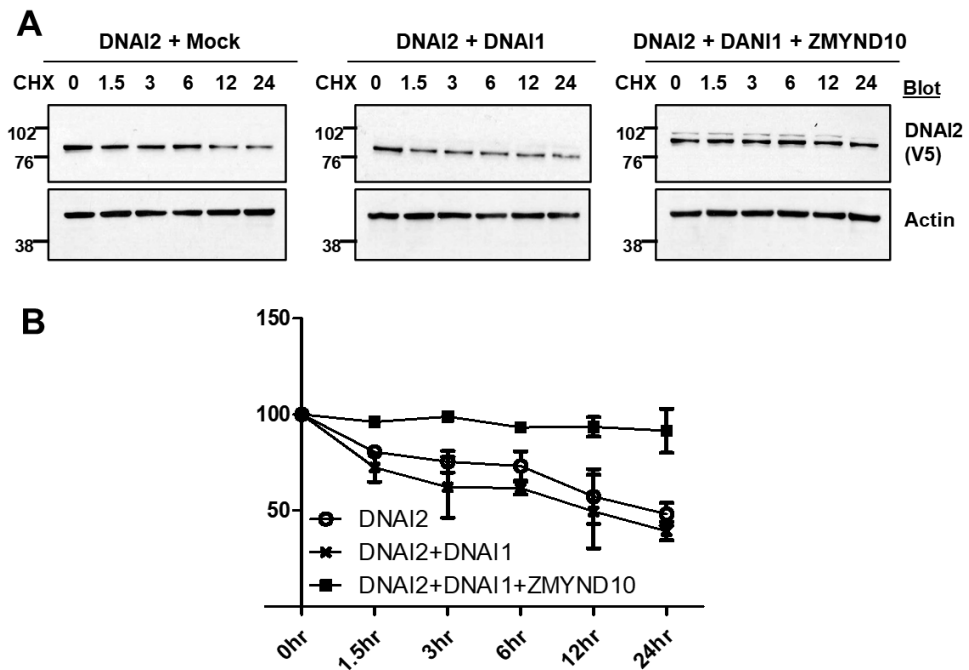


Figure 11. DNAI2 was stabilized by coexpression of both DNAI1 and ZMYND10. The stability of DNAI2 was examined using protein stability assay in HEK293T cells. After treated with cycloheximide (100 μ g/ml), protein samples were harvested at the indicated times. (A) DNAI2 was stabilized when coexpressed with both DNAI1 and ZMYND10. (B) The graph showed band intensities and is summarized from triplicate experiments.

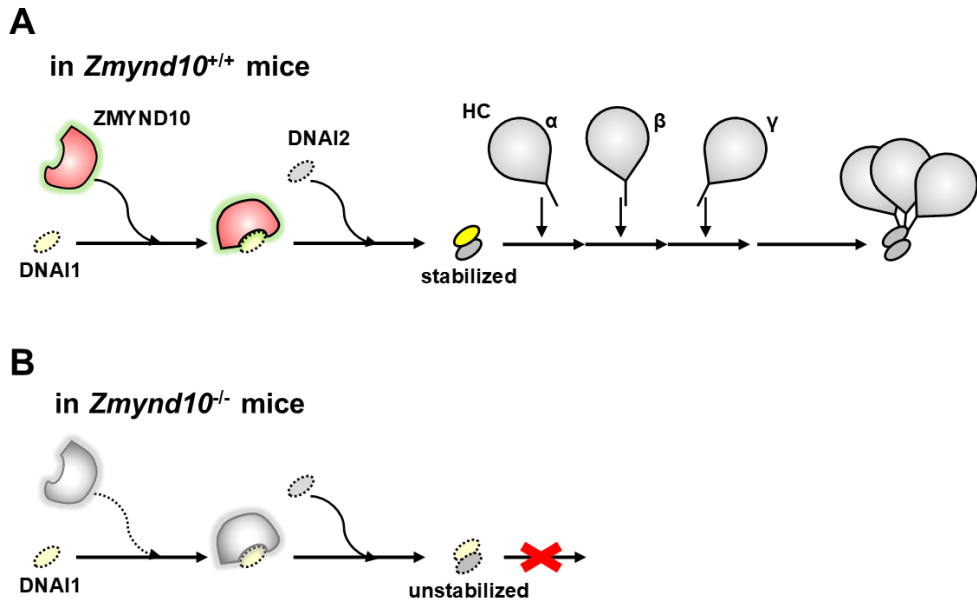


Figure 12. Function of ZMYND10 in the cytoplasmic preassembly of dynein arms. (A) ZMYND10 bound to and stabilizes DNAI1. DNAI1 formed a complex with DNAI2 before heavy chain proteins were attached to the intermediate chain complex. ZMYND10 may also regulate proper folding of DNAI1 or the assembly of intermediate chain complex. (B) In the absence of ZMYND10, both DNAI1 and DNAI2 were unstable and degraded.

IV. DISCUSSION

We generated a *Zmynd10*^{-/-} mice that demonstrate the symptoms of human PCD. The mice showed loss of ciliary motility and ODA and IDA components while ciliogenesis was maintained normally. They recapitulated the phenotype associated with ZMYND10 mutation and served as an appropriate model for studying PCD pathogenesis.

The assembly of dynein arms contains a number of regulatory factors including DNAAFs and chaperones that stabilize the dynein arm components,^{14,23,28} help proper folding and then contribute to the preassembly.²⁸ During the preassembly of ODA, HCs such as DNAH5 and DNAH11 are linked to ICs, DNAI1 and DNAI2. There are at least two steps of cytoplasmic preassembly of dynein HCs. The first step involves the folding of the dynein head domain which is required for HC stability. DNAAF1, DNAAF3 and DNAAF4 contribute to this step together with HSP70. The second step involves formation of the HC-IC complex and dissociation of chaperone involved in assembly, and require DNAAF3.¹⁴ IC-HC assembly fails when there is no IC subunit.¹¹ Down-regulation of DNAI1 and DNAI2 in *Zmynd10*^{-/-} mice indicate that ZMYND10 stabilizes these two proteins or mediates their assembly. Because the formation of IC complexes occurs prior to IC-HC assembly, reduced levels of DNAI1 and DNAI2 may account for the reduction of the ODA component, DNAH5. (Fig. 10C and D).

In this study, we showed that ZMYND10 forms a cytoplasmic protein network including LRRC6, C21ORF59, DYX1C1, IQUB and REPTIN. ZMYND10 is associated with REPTIN, but the expression level of various dynein arm components and ZMYND10 interactors did not decrease in *Zmynd10*^{-/-} mice (Fig. 7 and Fig. 10F-H). DYX1C1 interacts with KTU, HSP70 and HSP90,^{13,15} while REPTIN interacts with protein interacting with HSP90 (PIH) 1D1.²⁹ PIH1D3 interacts with KTU, DYX1C1, and HSP90,^{23,24} and is involved in the formation of IC complexes. Pih1d3 is known to maintain the stability of the IC1-IC2 complex by directly interacting with

the complex. Pih1d3 can promote the formation of the IC-HC complex, and the absence of Pih1d3 may indirectly reduce levels of Dnaic and Dnahc proteins in the mouse testis.²³

ZMYND10 is functionally similar to PIH1D3 in that both proteins interact with DYX1C1. IC is also reduced in mice without Zmynd10 or Pih1d3. The difference is that ZMYND10 primarily acts on DNAI1, while PIH1D3 is not well known.

In conclusion, our results indicate that many cytoplasmic proteins, including ZMYND10, organize a protein network in motile ciliated cells that control various aspects of the dynein arm preassembly with chaperone. ZMYND10 works in the early stages of this process, specifically controlling IC assembly by regulating DNAI1 stability or folding (Fig. 12). These results provide insights into the molecular mechanisms involved in dynein arm assembly and the pathogenesis of PCD-related defects.

V. CONCLUSION

In this study, I demonstrated that ZMYND10 regulates the assembly of the intermediate chain proteins which is the early process of cytoplasmic preassembly of dynein arms. ZMYND10 forms protein networks with the dynein arm components and dynein arm assembly factors for dynein arm assembly.

Our results revealed the molecular mechanisms of the dynein arm assembly and the pathogenesis of PCD-related defects. This study also suggests that the dynein arm assembly is strictly regulated from the beginning step.

REFERENCES

1. Leigh MW, Pittman JE, Carson JL, Ferkol TW, Dell SD, Davis SD, *et al.* Clinical and genetic aspects of primary ciliary dyskinesia/Kartagener syndrome. *Genetics in medicine : official journal of the American College of Medical Genetics* **11**, 473-487 (2009).
2. Shapiro AJ, Davis SD, Ferkol T, Dell SD, Rosenfeld M, Olivier KN, *et al.* Laterality defects other than situs inversus totalis in primary ciliary dyskinesia: insights into situs ambiguus and heterotaxy. *Chest* **146**, 1176-1186 (2014).
3. Horani A, Ferkol TW, Dutcher SK, Brody SL. Genetics and biology of primary ciliary dyskinesia. *Paediatric respiratory reviews* **18**, 18-24 (2016).
4. Ibanez-Tallon I, Heintz N, Omran H. To beat or not to beat: roles of cilia in development and disease. *Human molecular genetics* **12 Spec No 1**, R27-35 (2003).
5. Mazor M, Alkrinawi S, Chalifa-Caspi V, Manor E, Sheffield VC, Aviram M, *et al.* Primary ciliary dyskinesia caused by homozygous mutation in DNAL1, encoding dynein light chain 1. *American journal of human genetics* **88**, 599-607 (2011).
6. Pennarun G, Escudier E, Chapelin C, Bridoux AM, Cacheux V, Roger G, *et al.* Loss-of-function mutations in a human gene related to *Chlamydomonas reinhardtii* dynein IC78 result in primary ciliary dyskinesia. *American journal of human genetics* **65**, 1508-1519 (1999).
7. Loges NT, Olbrich H, Fenske L, Mussaffi H, Horvath J, Fliegauf M, *et al.* DNAI2 mutations cause primary ciliary dyskinesia with defects in the outer dynein arm. *American journal of human genetics* **83**, 547-558 (2008).
8. Olbrich H, Häffner K, Kispert A, Völkel A, Volz A, Sasmaz G, *et al.* Mutations in DNAH5 cause primary ciliary dyskinesia and randomization of left-right asymmetry. *Nature genetics* **30**, 143-144 (2002).

9. Bartoloni L, Blouin JL, Pan Y, Gehrig C, Maiti AK, Scamuffa N, *et al.* Mutations in the DNAH11 (axonemal heavy chain dynein type 11) gene cause one form of situs inversus totalis and most likely primary ciliary dyskinesia. *Proceedings of the National Academy of Sciences of the United States of America* **99**, 10282-10286 (2002).
10. Li Y, Onuoha EO, Damerla RR, Francis R, Furutani Y, Tariq M, *et al.* DNAH6 and Its Interactions with PCD Genes in Heterotaxy and Primary Ciliary Dyskinesia. *PLoS genetics* **12**, e1005821 (2016).
11. Fowkes ME, Mitchell DR. The Role of Preassembled Cytoplasmic Complexes in Assembly of Flagellar Dynein Subunits. *Molecular Biology of the Cell* **9**, 2337-2347 (1998).
12. Loges NT, Olbrich H, Becker-Heck A, Häffner K, Heer A, Reinhard C, *et al.* Deletions and point mutations of LRRC50 cause primary ciliary dyskinesia due to dynein arm defects. *American journal of human genetics* **85**, 883-889 (2009).
13. Omran H, Kobayashi D, Olbrich H, Tsukahara T, Loges NT, Hagiwara H, *et al.* Ktu/PF13 is required for cytoplasmic pre-assembly of axonemal dyneins. *Nature* **456**, 611-616 (2008).
14. Mitchison HM, Schmidts M, Loges NT, Freshour J, Dritsoula A, Hirst RA, *et al.* Mutations in axonemal dynein assembly factor DNAAF3 cause primary ciliary dyskinesia. *Nature genetics* **44**, 381-389, S381-382 (2012).
15. Tarkar A, Loges NT, Slagle CE, Francis R, Dougherty GW, Tamayo JV, *et al.* DYX1C1 is required for axonemal dynein assembly and ciliary motility. *Nature genetics* **45**, 995-1003 (2013).
16. Horani A, Ferkol TW, Shoseyov D, Wasserman MG, Oren YS, Kerem B, *et al.* LRRC6 Mutation Causes Primary Ciliary Dyskinesia with Dynein Arm Defects. *PloS one* **8**, e59436 (2013).
17. Kott E, Duquesnoy P, Copin B, Legendre M, Dastot-Le Moal F, Montantin G, *et al.* Loss-of-Function Mutations in LRRC6, a Gene Essential for Proper Axonemal Assembly of Inner and Outer Dynein Arms, Cause Primary Ciliary Dyskinesia. *American journal of human genetics* **91**, 958-964 (2012).

18. Zariwala Maimoona A, Gee HY, Kurkowiak M, Al-Mutairi DA, Leigh MW, Hurd TW, *et al.* ZMYND10 Is Mutated in Primary Ciliary Dyskinesia and Interacts with LRRC6. *The American Journal of Human Genetics* **93**, 336-345 (2013).
19. Moore DJ, Onoufriadis A, Shoemark A, Simpson MA, zur Lage PI, de Castro SC, *et al.* Mutations in ZMYND10, a gene essential for proper axonemal assembly of inner and outer dynein arms in humans and flies, cause primary ciliary dyskinesia. *American journal of human genetics* **93**, 346-356 (2013).
20. Austin-Tse C, Halbritter J, Zariwala MA, Gilberti RM, Gee HY, Hellman N, *et al.* Zebrafish Ciliopathy Screen Plus Human Mutational Analysis Identifies C21orf59 and CCDC65 Defects as Causing Primary Ciliary Dyskinesia. *American journal of human genetics* **93**, 672-686 (2013).
21. Hjeij R, Lindstrand A, Francis R, Zariwala MA, Liu X, Li Y, *et al.* ARMC4 mutations cause primary ciliary dyskinesia with randomization of left/right body asymmetry. *American journal of human genetics* **93**, 357-367 (2013).
22. Horani A, Druley TE, Zariwala MA, Patel AC, Levinson BT, Van Arendonk LG, *et al.* Whole-exome capture and sequencing identifies HEATR2 mutation as a cause of primary ciliary dyskinesia. *American journal of human genetics* **91**, 685-693 (2012).
23. Olcese C, Patel MP, Shoemark A, Kiviluoto S, Legendre M, Williams HJ, *et al.* X-linked primary ciliary dyskinesia due to mutations in the cytoplasmic axonemal dynein assembly factor PIH1D3. *Nature communications* **8**, 14279 (2017).
24. Paff T, Loges NT, Aprea I, Wu K, Bakey Z, Haarman EG, *et al.* Mutations in PIH1D3 Cause X-Linked Primary Ciliary Dyskinesia with Outer and Inner Dynein Arm Defects. *American journal of human genetics* **100**, 160-168 (2017).
5. Liu Y, Chen W, Gaudet J, Cheney MD, Roudaia L, Cierpicki T, *et al.* Structural basis for recognition of SMRT/N-CoR by the MYND domain and its contribution to AML1/ETO's activity. *Cancer cell* **11**, 483-497 (2007).

26. McClintock TS, Glasser CE, Bose SC, Bergman DA. Tissue expression patterns identify mouse cilia genes. *Physiological Genomics* **32**, 198-206 (2008).
27. Zhao L, Yuan S, Cao Y, Kallakuri S, Li Y, Kishimoto N, *et al.* Reptin/Ruvbl2 is a Lrrc6/Seahorse interactor essential for cilia motility. *Proceedings of the National Academy of Sciences of the United States of America* **110**, 12697-12702 (2013).
28. Kobayashi D, Takeda H. Ciliary motility: the components and cytoplasmic preassembly mechanisms of the axonemal dyneins. *Differentiation; research in biological diversity* **83**, S23-29 (2012).
29. Yamamoto R, Hirono M, Kamiya R. Discrete PIH proteins function in the cytoplasmic preassembly of different subsets of axonemal dyneins. *The Journal of cell biology* **190**, 65-71 (2010).
30. Dong F, Shinohara K, Botilde Y, Nabeshima R, Asai Y, Fukumoto A, *et al.* Pih1d3 is required for cytoplasmic preassembly of axonemal dynein in mouse sperm. *The Journal of cell biology* **204**, 203-213 (2014).
31. Inaba Y, Shinohara K, Botilde Y, Nabeshima R, Takaoka K, Ajima R, *et al.* Transport of the outer dynein arm complex to cilia requires a cytoplasmic protein Lrrc6. *Genes to cells : devoted to molecular & cellular mechanisms* **21**, 728-739 (2016).
32. Matsuo M, Shimada A, Koshida S, Saga Y, Takeda H. The establishment of rotational polarity in the airway and ependymal cilia: analysis with a novel cilium motility mutant mouse. *American journal of physiology Lung cellular and molecular physiology* **304**, L736-745 (2013).
33. You Y, Brody SL. Culture and differentiation of mouse tracheal epithelial cells. *Methods in molecular biology (Clifton, NJ)* **945**, 123-143 (2013).
34. Vladar EK, Brody SL. Analysis of ciliogenesis in primary culture mouse tracheal epithelial cells. *Methods in enzymology* **525**, 285-309 (2013).

ABSTRACT (in Korean)

Multiciliated cell에서 dynein arm의 세포질 preassembly에 있어서 ZMYND10의 역할

<지도교수 지 현 영>

연세대학교 대학원 의과학과

조 경 지

Zinc finger MYND-type-containing(ZMYND)10은 섬모 세포에서 발현되는 세포질 단백질이다. ZMYND10에 돌연변이가 생기면 원발성 섬모 운동 이상증 (Primary Ciliary Dyskinesia; PCD)을 유발한다고 알려져 있지만, ZMYND10의 구체적인 기능과 PCD 를 일으키는 기전은 제대로 이해되지 않고 있다.

이를 밝혀내기 위해 *Zmynd10*^{-/-} (*Zmynd10* KO) 마우스를 제작하였고, 이 마우스는 수두증과 내장전위증을 비롯한 전형적인 PCD 와 유사한 표현형을 보였다. 돌연변이 마우스에서 운동성 섬모의 형태와 수는 물론, 9+2 axoneme 구조도 정상이었다. 그러나 섬모의 움직임에 필요한 multisubunit 인 dynein arm 에 결함이 있었다. ZMYND10은 dynein arm 의 세포질 preassembly 에 관여하는 단백질, 그리고 outer dynein arm 구성요소와 단백질 상호작용을 하였다. *Zmynd10*^{-/-} 마우스에서는 ZMYND10과 상호작용하는 단백질들과 dynein arm 구성요소들의 단백질 양이 현저하게 감소하였다. LRRC6와 DNAI1은 ZMYND10과 동시에 발현되었을 때

ZMYND10에 의해 안정화되었다. DNAI2는 DNAI1과 ZMYND10과 함께 발현될 때 더 안정적이었는데, 이는 ZMYND10이 DNAI1을 안정화시킴으로써 intermediate chain complex의 assembly를 조절한다는 것을 암시한다.

이와 같은 결과는 ZMYND10이 세포질에서 complex를 형성하고, ZMYND10이 포함된 이 complex가 dynein arm의 intermediate chain 단백질이 세포질에서 preassembly되는 과정을 조절한다는 것을 보여준다.

핵심되는 말: 운동성 섬모, 원발성 섬모 운동 이상증 (PCD), dynein arm, cytoplasmic preassembly, ZMYND10

PUBLICATION LIST

- Heon Yung Gee*, Carolin E. Sadowski*, Pardeep K. Aggarwal, Jonathan D. Porath, Toma A. Yakulov, Markus Schueler, Syjetlana Lovric, Shazia Ashraf, Daniela A. Braun, Jan Halbritter, Humphrey Fang, Rannar Airik, Virginia Vega-Warner, Kyeong Jee Cho, et al. FAT1 mutations cause a glomerulotubular nephropathy. Nat Commun. 2016 Feb 24;7:10822. doi: 10.1038/ncomms10822.
- Hyo Jin Park*, Tae Hee Kim*, So Won Kim, Shin Hye Noh, Kyeong Jee Cho, et al. Functional characterization of *ABCB4* mutations found in progressive familial intrahepatic cholestasis type 3. Sci Rep. 2016 Jun 3;6:26872. doi: 10.1038/srep26872.
- Jinsei Jung*, Joon Suk Lee*, Kyeong Jee Cho, et al. Genetic Predisposition to Sporadic Congenital Hearing Loss in a Pediatric Population. Sci Rep. 2017 Apr 6;7:45973. doi: 10.1038/srep45973.